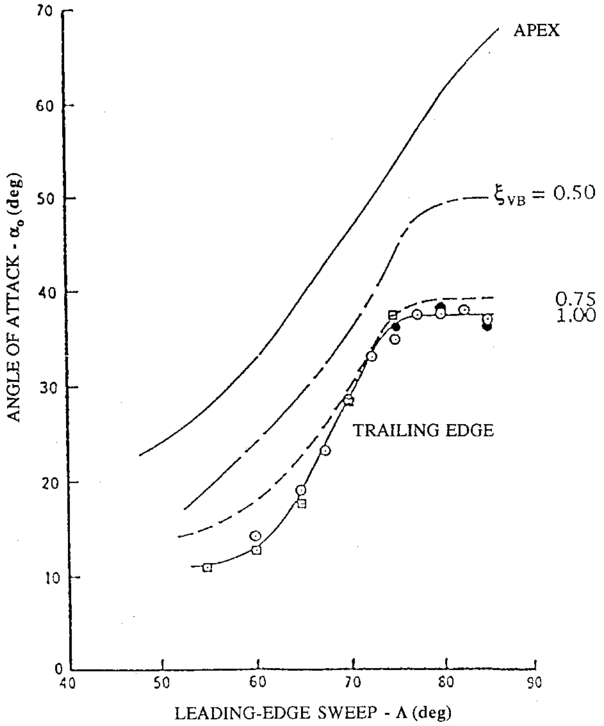

Fig. 6 Vortex breakdown position on sharp-edged delta wings.[14]

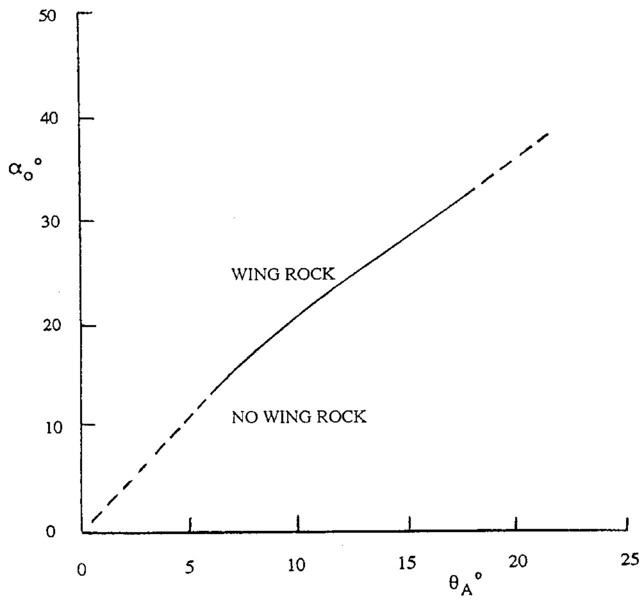

Fig. 7 Predicted wing-rock boundary for slender delta wings.

Conclusions

The information that the vehicle designer needs early in the design cycle is 1) the angle-of-attack/leading-edge-sweep range in which slender wing rock will occur and 2) the maximum wing-rock amplitude. Figure 7 provides the (α, θ_A) boundary for starting wing rock. To determine the maximum possible oscillation amplitude, one needs to repeat the computations,[11] producing Fig. 5 for apex half-angles θ_A different from 10 deg.

References

[1]Nguyen, L. T., Yip, L., and Chambers, J. R., "Self-Induced Wing Rock of Slender Delta Wings," AIAA Paper 81-1883, Aug. 1981.

[2]Levin, D., and Katz, J., "Dynamic Load Measurements with Delta Wings Undergoing Self-Induced Roll Oscillations," *Journal of Aircraft*, Vol. 21, No. 1, 1984, pp. 30–36.

[3]Arena, A. S., Jr., and Nelson, R. C., "The Effect of Asymmetric Vortex Wake Characteristics on a Slender Delta Wing Undergoing Wing Rock Motion," AIAA Paper 89-3348, Aug. 1989.

[4]Arena, A. S., Jr., Nelson, R. C., and Schiff, L. B., "An Experimental Study of the Nonlinear Phenomenon Known as Wing Rock," AIAA Paper 90-2812, Aug. 1990.

[5]Arena, A. S., Jr., and Nelson, R. C., "Unsteady Surface Measurements on a Slender Delta Wing Undergoing Limit Cycle Wing Rock," AIAA Paper 91-0434, Jan. 1991.

[6]Arena, A. S., Jr., and Nelson, R. C., "A Discrete Vortex Model for Predicting Wing Rock of Slender Wings," AIAA Paper 92-4497, Aug. 1992.

[7]Arena, A. S., Jr., and Nelson, R. C., "Experimental Investigations on Limit Cycle Wing Rock of Slender Wings," *Journal of Aircraft*, Vol. 31, No. 5, 1994, pp. 1148–1155.

[8]Ericsson, L. E., and Beyers, M. E., "Ground Facility Interference Effects on Slender Vehicle Unsteady Aerodynamics," *Journal of Aircraft*, Vol. 33, No. 1, 1996, pp. 117–124.

[9]Ericsson, L. E., and King, H. H. C., " Rapid Prediction of High-Alpha Unsteady Aerodynamics of Slender-Wing Aircraft," *Journal of Aircraft*, Vol. 29, No. 1, 1992, pp. 85–92.

[10]Ericsson, L. E., "Fluid Dynamics of Slender Wing Rock," *Journal of Aircraft*, Vol. 21, No. 5, 1984, pp. 322–328.

[11]Ericsson, L. E, "Analytic Prediction of the Maximum Amplitude of Slender Wing Rock," *Journal of Aircraft*, Vol. 26, No. 1, 1989, pp. 35–39.

[12]Ericsson, L. E, "Unsteady Aerodynamics of Separating and Reattaching Flow on Bodies of Revolution," *Recent Research on Unsteady Boundary Layers*, Vol. 1, IUTAM Symposium, Laval Univ., PQ, Canada, 1971, pp. 481–512.

[13]Polhamus, E. C., "Prediction of Vortex-Lift Characteristics by a Leading-Edge Suction Analogy," *Journal of Aircraft*, Vol. 8, No. 4, 1971, pp. 193–199.

[14]Wentz, W. H., and Kohlman, D. L., "Vortex Breakdown on Slender Sharp-Edged Wings," *Journal of Aircraft*, Vol. 8, No. 3, 1971, pp. 156–161.

[15]Stahl, W., Mahmod, M., and Asghar, A., "Experimental Investigation of the Vortex Flow on Delta Wings at High Incidence," *AIAA Journal*, Vol. 30, No. 4, 1992, pp. 1027–1032.

[16]Ericsson. L. E., "Slender Wing Rock Revisited," *Journal of Aircraft*, Vol. 30, No. 3, 1993, pp. 352–356.

Correlation for the Estimation of Afterbody Drag with Hot Jet Exhaust

N. B. Mathur*
National Aerospace Laboratories, Bangalore 560 017, India

Introduction

MODERN turbojet and turbofan engines of combat aircraft operating over a wide range of power settings experience jet exhaust temperature typically varying from 1000–2000 K, whereas much of afterbody-nozzle testing is conducted with a cold jet near 300 K.[1–5] Thus there remains a problem to determine the extent to which jet total temperature (and its associated gas constants) affects the afterbody drag of a combat aircraft under various operating conditions of its nozzle during the flight operation.[6–8] Physical modeling of jet freestream interactions with temperature effects is quite difficult; and, calculations of afterbody drag with hot jet exhaust are computationally intensive. Efforts made earlier for the es-

Received Aug. 17, 1997; revision received June 6, 1998; accepted for publication June 13, 1998.

*Scientist, Experimental Aerodynamics Division. Member AIAA.

Table 1 Afterbody tests with hot jet exhaust: AEDC and NASA experiments

Experiments	AEDC	NASA
Wind tunnel	16 ft, PWT	Langley, 16 ft
Maximum diameter of afterbody model	250 mm	152 mm
d_b/d_m	0.42	0.51
d_j/d_m	0.40	0.50
Boat-tail angle (β)	10, 15, and 25 deg	10 and 20 deg
Freestream Mach number (M_∞)	0.6–1.5	0.6–1.2
Reynolds number ($Re_{N,m} \times 10^{-6}$)	4–16	10–14
Nozzle	Convergent	Convergent and convergent–divergent
Jet Mach number (M_j)	$M_j = 1$	$M_j = 1$ and 2
Hot jet generation	Ethylene–air combustor housed inside model	Decomposition of hydrogen peroxide inside model
Jet pressure ratios (P_{0j}/p_∞)	Jet-off to 8.0	Jet-off to 20.0
Jet plume temperature (T_{0j}, K)	300, 1165, 1580	300, 646, 1013
Specific heat ratio of jet exhaust (γ_j)	1.40, 1.30, 1.28	1.40, 1.30, 1.26

Notes: d_m, d_b, and d_j are forebody (maximum), base, and jet diameters, respectively. Re_N is Reynolds number/meter. P_{0j} and p_∞ are stagnation pressure of jet and freestream static pressure, respectively.

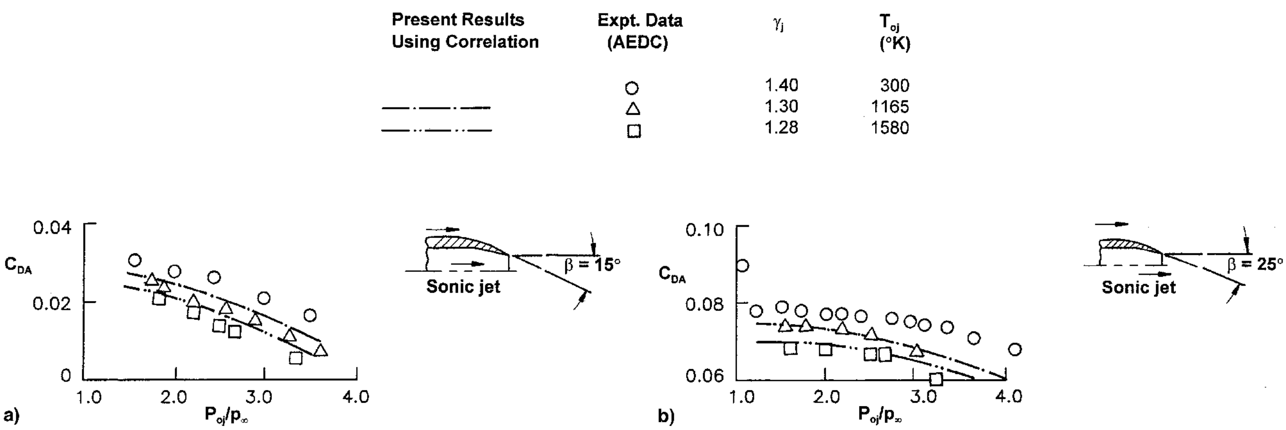

Fig. 1 Estimation of afterbody drag with sonic hot jet exhaust, M_∞ = 0.60. β = a) 15 and b) 25 deg.

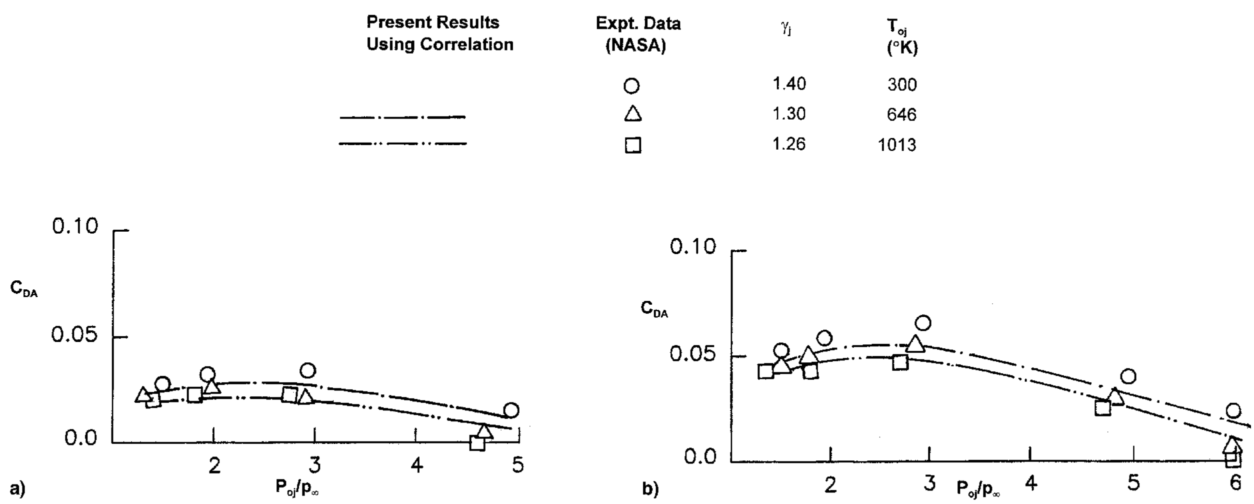

Fig. 2 Estimation of afterbody drag with sonic hot jet exhaust: a) M_∞ = 0.80, β = 20 deg and b) M_∞ = 0.90, β = 20 deg.

timation of afterbody drag with hot jet exhaust had limited success.[1,9,10] In the present analysis, a simple correlation is proposed that can be used in the subsonic and transonic Mach number range for the estimation of afterbody pressure drag with jet temperature effects.

Proposed Correlation of Afterbody Drag with Jet Temperature Effects

Afterbody drag characteristics with an underexpanded jet are influenced predominantly by its jet plume displacement effects.[4–8] Because the specific heat ratio of hot jet (γ_{jh}) is less than that of cold air jet (γ_{jc} = 1.4), jet plume displacement effects on afterbody drag are relatively larger in the presence of hot jet exhaust than that with the cold jet at the same jet pressure ratio. Hence, if the relative displacement effects of the hot and cold jet could be assessed, it would be possible to estimate, grossly, the jet temperature effects on drag from cold jet test data.

Based on an analysis of the available hot jet test data and experience gained during the cold and hot jet experiments con-

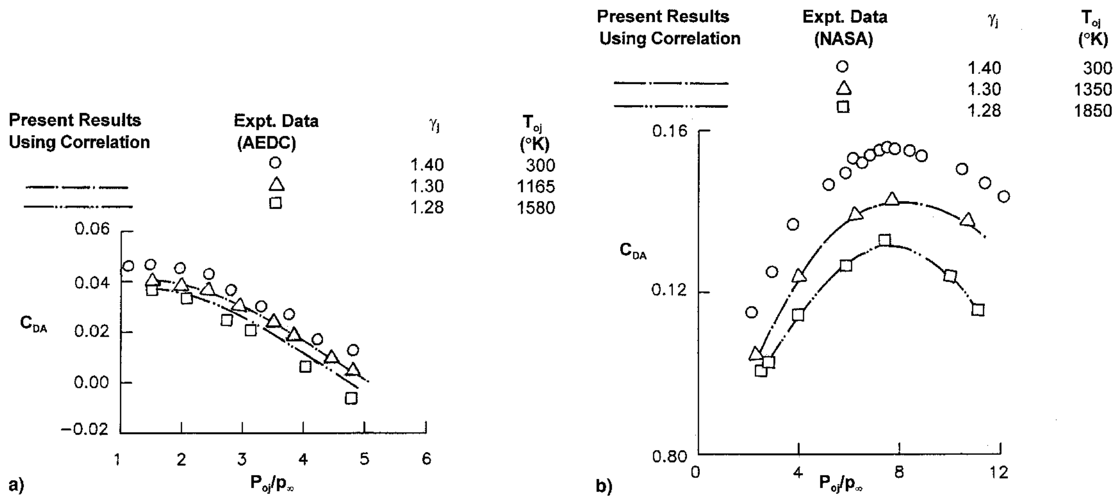

Fig. 3 Estimation of afterbody drag with sonic hot jet exhaust, $M_\infty = 0.90$. β = a) 15 and b) 25 deg.

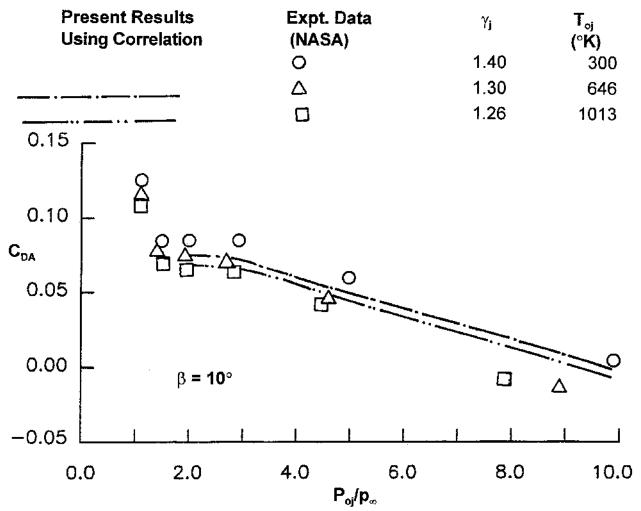

Fig. 4 Estimation of afterbody drag with sonic hot jet exhaust, $M_\infty = 0.95$.

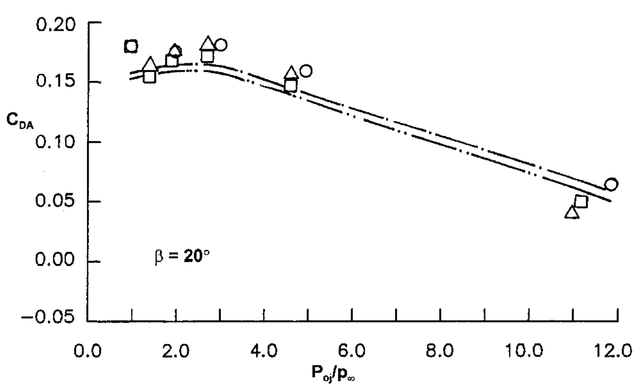

Fig. 5 Estimation of afterbody drag with sonic hot jet exhaust, $M_\infty = 1.20$.

ducted earlier at National Aerospace Laboratories (NAL),[4,11] an empirical correlation for the estimation of afterbody drag with hot jet exhaust is suggested. It is based on the specific heat ratios of cold and hot jet exhaust. The afterbody drag coefficient with hot jet exhaust $[C_{DA(h)}]$ is given by

$$C_{DA(h)} = C_{DA(c)}/(\gamma_{jc}/\gamma_{jh})^2$$

where $C_{DA(c)}$ is the afterbody drag (sum of boat-tail and base drag) with cold jet exhaust; γ_{jc} is the specific heat ratio of cold jet at a total temperature (T_{0j}) of 300K; and γ_{jh} is the specific heat ratio of the hot jet exhaust.

Validation

To demonstrate the usefulness of the preceding correlation, afterbody drag data,[12–14] obtained from tests at the Arnold Engineering and Development Center (AEDC), and NASA wind tunnels on boat-tailed afterbody configurations with sonic jet exhaust have been used. The jet total temperature involved in these experiments were in the range of 300–1600 K (Table 1). The values of γ_{jc} and γ_{jh} for these cases have been taken from the respective publications and are reproduced in Table 1.

Considering the simplicity of the approach, estimates of afterbody drag with jet temperature effects using the preceding correlation show, in general, good agreement (Figs. 1–5) with the hot jet test data generated in AEDC and NASA tunnels. This correlation has been validated against available test data at subsonic and transonic Mach numbers with sonic hot jet (Figs. 1–5) on contoured boat-tailed afterbodies having negligible base thickness and boat-tail angle (β) in the range of 10–25 deg.

Conclusions

A simple correlation is proposed for the estimation of afterbody drag with hot jet exhaust from the cold jet test data. Good agreement with the available drag data with sonic hot jet exhaust is observed and the proposed correlation may be very useful during preliminary design phase of combat aircraft. The correlation is now being extended to estimate the afterbody drag in the supersonic freestream Mach number range and with supersonic hot jet exhaust.

Acknowledgment

The author is very grateful to P. R. Viswanath, Head of the Experimental Aerodynamics Division, for his valuable suggestions during the preparation and progress of this work.

References

[1]Carter, E. C., "Aerodynamics of Aircraft Afterbody: Jet Simulation," AGARD AR 226, June 1986.

[2]Compton, W. B., "An Experimental Study of Jet Exhaust Simulation," AGARD CP150-16, March 1975; also NASA TMX-71975, June 1974.

[3]Aulehla, F., and Latter, K., "Nozzle/Airframe Interference and Integration," AGARD LS-53, May 1972.

[4]Mathur, N. B., and Yajnik, K. S., "Underexpanded Jet-Freestream Interactions on an Axisymmetric Afterbody Configuration," *AIAA Journal*, Vol. 28, No. 1, 1990, pp. 47–50.

[5]Mathur, N. B., "Effects of Underexpanded Jet on Afterbody Drag of an Axisymmetric Afterbody Configuration," National Aerospace Labs., FM TM 84-2, 1984.

[6]Peters, W. L., "An Evaluation of Jet Simulation Parameters for Nozzle Afterbody Testing at Transonic Mach Numbers," Arnold Engineering Development Center, TR-76-109, Oct. 1976.

[7]Robinson, C. E., High, M. D., and Thompson E. P., "Exhaust Plume Temperature Effects on Nozzle Afterbody Performance over the Transonic Mach Number Range," AGARD, CP150-19, March 1975.

[8]Robinson, C. E., and High, M. D., "Exhaust Plume Temperature Effects on Nozzle Afterbody Performance over the Transonic Mach Number Range," Arnold Engineering Development Center, TR-74-9, 1974.

[9]Price, E. A., and Peters, W. L., "Test Techniques for Jet Effects on Fighter Aircraft," AGARD, CP-348-24, 1984.

[10]Zacharias, A., "An Experimental and Theoretical Investigation of the Interaction Between the Engine Jet and Surrounding Flow Field," AGARD, CP-308, Jan. 1982. (Paper 8).

[11]Mathur, N. B., and Yajnik, K. S., "Jet Plume Temperature Effects on Afterbody Pressure Distribution and Drag," *International Journal of Turbo and Jet Engines*, Vol. 3, 1986, pp. 91–97.

[12]Galigher L. L., Yaros, S. F., and Bauer R. C., "Evaluation of Boat-Tail Geometry and Exhaust Plume Temperature Effects on Nozzle Afterbody Drag at Transonic Mach Numbers," Arnold Engineering Development Center, TR 76-102, Oct. 1977.

[13]Peters, W. L., and Kennedy T. L., "An Evaluation of Jet Simulation Parameter for Nozzle/Afterbody Testing at Transonic Mach Numbers," AIAA Paper 77-106, 1977.

[14]Compton, W. B., "Effects of Jet Exhaust Gas Properties on Exhaust Simulation and Afterbody Drag," NASA TR-R 444, Oct. 1975.

Lift Enhancement of a Wing/Strake Configuration Using Pneumatic Blowing

Richard M. Howard,* James G. Willson,† and Craig J. Zgraggen‡
U.S. Naval Postgraduate School, Monterey, California 93943

Introduction

THE maintenance of air superiority in the future will depend upon the ability to perform rapid transient maneuvers at high angles of attack (AOAs), often into the poststall flight regime. Techniques for enhanced lift and control at high AOA are being explored to meet this need. Current-generation fighters often employ strakes for vortex lift; however, at some angle of attack, the strake vortex bursts, reducing the effective lift as well as possibly leading to yaw control loss and tail structural problems.

One technique under study for both yaw control and increased lift is the use of pneumatic blowing, either on the aircraft forebody,[1,2] at the wing leading edge,[3] or over the lifting surface.[4,5] Cornelius et al.[1] studied the effects of various nozzle geometries for blowing at the forebody of an X-29 model, and found that a nozzle orientation of 60 deg in from the longitudinal axis produced the largest yawing moments in manipulating the forebody vortices. Celik and Roberts[3] considered forebody-slot and wing-slot blowing for a delta-wing ogive-nose configuration and noted that forebody blowing produced rolling moments four times greater than with tangential wing blowing. LeMay and Rogers[4] conducted a water-tunnel study of the effects of blowing on strake/wing-vortex coupling. Vortex breakdown was delayed past an AOA of 36 deg from a blowing port at the midstrake position. All blowing did not produce favorable results; blowing from ports aft of the strake–wing junction sometimes led to earlier vortex breakdown. Roach and Kuhlman[5] mapped strake vortices using laser-light-sheet and laser-Doppler-anemometry methods. Reductions in vortex coupling and delays in vortex breakdown were noted in particular for blowing from the forward port locations slightly behind the strake apex. Johari and Moreira[6] studied the enhanced effects of pulsed blowing during ramped pitching.

Past efforts in analyzing the effect of blowing over a strake–wing configuration have involved flow visualization and flowfield measurements. Though progress has been made toward identifying flow mechanisms responsible for vortex-breakdown delay and vortex relocation, few measurements of the global effects on the actual lift and drag have been noted. This study treats those effects. Comparisons involve variations in blowing port position, blowing coefficient, blowing sweep angle, and blowing inclination angle.

Experiment

A test was performed with a half-model used in conjunction with a reflection-plane external balance in a low-speed wind tunnel. The three-component balance is an external column strain-gauge balance attached to a turntable mounted flush with the reflection plane. The reflection plane and balance are designed to accommodate half models oriented in the vertical plane. Figure 1 shows a side view of the model mounted in the wind tunnel. The model was comprised of a half-fuselage with ogive forebody, a 36-deg-sweep wing using an NACA 64A008 airfoil, and a sharp 18-deg-wedge 76-deg-sweep strake. The general planform shape followed that of Kern,[7] though Kern's study used a flat plate with beveled edges. The wing had zero deg of incidence, dihedral, and twist.

Blowing ports 1 and 2 were located 0.235·mac and 0.329·mac aft of the strake apex, respectively [mac being the wing mean aerodynamic (geometric) chord]. The blowing tubes were 0.125-in. stainless-steel tubes. Tube 1 was bent (or swept, defined in the same manner as wing sweep) 30 deg, tube 2 was swept 45 deg, and tube 3 was swept 60 deg. Twisting each tube from −10 to 40 deg away from the strake surface allowed for the variation of tube inclination angle.

A mass flow meter was used to determine the blowing coefficient. Air was fed to the tubes from three storage tanks through a regulator at 65 psi. The air moved through urethane tubing to a plenum chamber inside the model before being fed

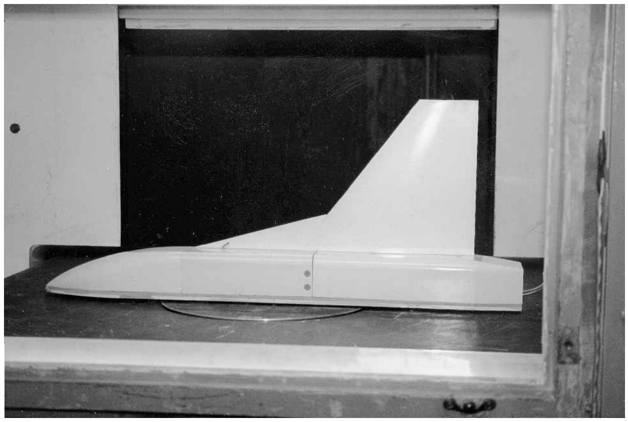

Fig. 1 Wing/strake model with blowing port (shown at port 1 location).

Received July 7, 1998; accepted for publication July 16, 1998. This paper is declared a work of the U.S. Government and is not subject to copyright protection in the United States.

*Associate Professor, Department of Aeronautics and Astronautics. Senior Member AIAA.

†Graduate Student, Aeronautical Engineering, Lieutenant, U.S. Navy. Member AIAA.

‡Graduate Student, Aeronautical Engineering, Lieutenant, U.S. Navy.